

# Optimizing stator/rotor pole ARC for torque and economy in electric vehicle switched reluctance motors

Saif Kh Al-Farhan, Omar Sharaf Al-Deen Yehya Al-Yozbak

Department of Electrical Engineering, College of Engineering, University of Mosul, Mosul, Iraq

## Article Info

### Article history:

Received Jan 30, 2023

Revised Apr 24, 2023

Accepted May 3, 2023

### Keywords:

Electric vehicles

Finite element analysis

Genetic algorithm

Optimization

Stator/rotor pole arc

Switched reluctance motor

## ABSTRACT

Numerous researchers as well as the vehicle industry are paying increasing attention to the switching reluctance motor (SRM) drive. Due to its specialized qualities, SRMs are commonly used in electric vehicle applications. The stator/rotor pole arc of an 8/6 SRM is included in this study's investigation of design principles and performance improvement for poles arcs variation. Several limitations for the stator/rotor pole arc angle are derived for the design principles. These concepts are addressed in the finite element (FE) analysis of SRM topological parameters used in conventional and optimization analysis. The stator/rotor polar arc is tuned for performance using a genetic algorithm (GA) in order to maximize torque and efficiency. An ideal solution is chosen when the optimization results are represented. The proposed method can increase the maximum and average torque with (27.24%, 35.98%, 49.42%, 60.14%), (12.59%, 45.19%, 47.87%, 48.92%) for speeds [900, 1500, 2250, 3000 (rpm)] respectively, As shown by the comparison between the conventional and optimal designs. As well as the efficiency is improved (0.35%, 0.61%, 1.08%, 1.28%) for speeds [900, 1500, 2250, 3000 (rpm)] respectively.

This is an open access article under the [CC BY-SA](https://creativecommons.org/licenses/by-sa/4.0/) license.



## Corresponding Author:

Omar Sharaf Al-Deen Yehya Al-Yozbak

Department of Electrical Engineering, College of Engineering, University of Mosul

Mosul, Iraq

Email: o.yehya@uomosul.edu.iq

## 1. INTRODUCTION

Due to environmental degradation and a lack of oil supplies, the development of electric vehicles (EVs) and hybrid electric vehicles (HEVs) is currently in high demand [1]–[3]. Switched reluctance machines (SRMs) have been anticipated to serve as a propulsion machine for EVs or HEVs. Because of the exceptional inborn qualities like accurate speed control and low cost [4], reliability, high fault tolerance, potential high temperature operation, and the benefit of being rare-earth-free. Switched reluctance motors are faster than stepper motors and don't require expensive permanent magnets. They also have the advantages of AC induction motors, DC motors, and brushless motors. For applications requiring greater torque density and variable speeds, the SRM is also a cost-effective substitute for traditional synchronous and induction machines [5]. Despite having positive characteristics, SRM has several unavoidable drawbacks, such as high torque ripple and an unbalanced radial force caused by a strong nonlinear step-by-step magnetic field [6]–[8]. In order to enhance the performance of the electrical machinery used in various applications, it is necessary to pay attention to them [9]. Where the impact of topology and current model-related characteristics on the functioning of electrical devices is researched, and created in accordance with guidelines that guarantee the avoidance of faults [10]. The electromagnetic capabilities of motors include torque ripple, efficiency or torque density, was the primary focus of earlier research on their design and optimization methods.

The article presents a practical method for raising increasing the number of rotor poles to increase the torque [11]. It leads to a bigger design and a higher machine cost. In order to enhance torque and decrease magnetic saturation, the rotor poles of SRM have been adjusted [12]. Using brief magnetic lines or other stimulation methods segmented stator or rotor topology is an effective way to increase torque output [13]–[15]. Nevertheless, it makes production more complicated and reduces precision. To improve torque performance, some altered SRM structures have also been proposed. include two layers for each phase [16] and axial type SRM [17], [18]. The examination of a two-tooth topology that has been improved to have more rotor teeth than stator teeth [19], But it is unsuitable for applications requiring high speed. In earlier investigations, a variety of optimization techniques for the motor's dimension, shape, and topology were used [20]. The parameterized geometry is also [21] was primarily constructed for optimizing topology and dimensions. The standard optimization method should include the following four steps: establishing the goals and limitations, specifying the search space, looking at the solution space, and assessing and interpreting the outcomes [22]. Choosing the suitable SRM structure for a specific application, such as an EV application, can be made more simpler and more efficient by taking into account the effects of SRM designs. According to traditional studies, the best machine configurations for EV application are SRM 8/6 and 12/8 [23]. By observing the torque per ampere values of the machines and taking into account the results of 6-phase and 4-phase SRM, the 4-phase machine is thought to be the best of the two. Nevertheless, these enhancements come at the expense of the electric machine and power electronics system becoming more complicated [23]. This study looked into how the 8/6 SRM 5 (Kw) 4-phase motor's stator/rotor pole arc affected torque and efficiency improvements via genetic algorithm (GA) optimization. Utilizing finite element (FE) analysis, the estimation and investigation of flux linkage and torque after the new topology has been optimized (FE) analysis. Then demonstrate why the proposed model's properties are superior to the standard model, they are compared. The rest of this essay is structured as follows. Significant research is presented in section 2. Working concepts for switching reluctance motors are presented in Section 3. Section 4 presents the mathematical model of SRM. The SRM's proposed design and general method are presented in section 5. Section 6 discuss the results of conventional and optimization parameters. Section 7 has the conclusion.

## 2. SIGNIFICANT OF STUDY

Switched reluctance machines (SRMs) have gained great importance in the application of EVs and HEVs compared to induction machines and permanent magnet machines. Due to its good characteristics of simple construction, low cost, high temperature and fault tolerance. However, it suffers from problems during normal operation, represented by high torque ripple, unbalanced radial force, and loud acoustic noise. These problems can be addressed through two methods: topology parameters optimization of the motor, and using current control techniques. Where the study focused on the treatment of motor problems by enhancing the topology parameters of SRM that change the shape of the stator/rotor pole, represented by the angles of the stator/rotor pole arc. As these parameters are considered the most influential on improving the torque and efficiency of SRM. The optimization of the genetic algorithm (GA) was used to choose the best values for the composition parameters, which contribute to improving the characteristics of SRM effectively to ensure that it works in the best way in the application of EVs and HEVs.

## 3. WORKING PRINCIPLES OF SWITCHED RELUCTANCE MOTOR

The SRM structure is simple because of its rotor design, which is depicted in Figure 1. There is no permanent magnet in the stator's configuration, which is made up of copper windings. Electronic power switches are used to supply windings to the stator poles, with the opposing poles supplying the same sequence of windings. The 8/6 arrangement of the research SRM's poles (eight stators and six rotor) is used.

Both the stator and rotor cores are made of steel. High nonlinearity and discreteness characterize the stator and rotor structures' torque output. According to Figure 2, the SRM moves the rotor to a position where the winding inductance is at its highest level. Rotor rotation is governed by the stator windings sequence of current commutation, in which the current is pulsed one-step at a time. This is accomplished via a universal control and converter drive system. SRM control is influenced by the variables turn-on/off angle, rotor position, and current [24].

Similar to a stepper motor with variable reluctance, the switched reluctance motor switches the phase current on and off while the rotor is at exact positions that can shift with speed and torque. Additionally, the rotor and stator both have noticeable poles. Figure 3 shows at various rotor locations and rated speed (3000 rpm), the link between flux and current performance in steady-state operation.

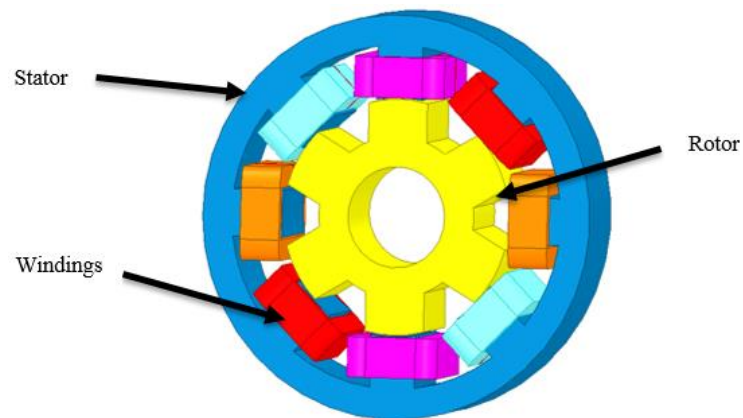


Figure 1. The traditional switching reluctance motor's construction

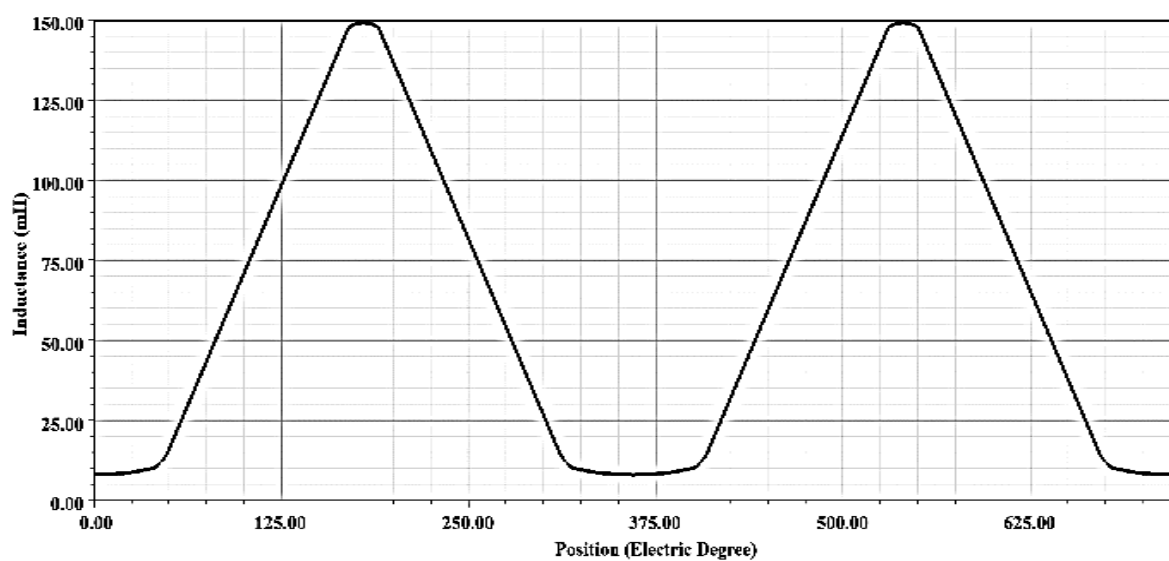


Figure 2. Variation of inductance

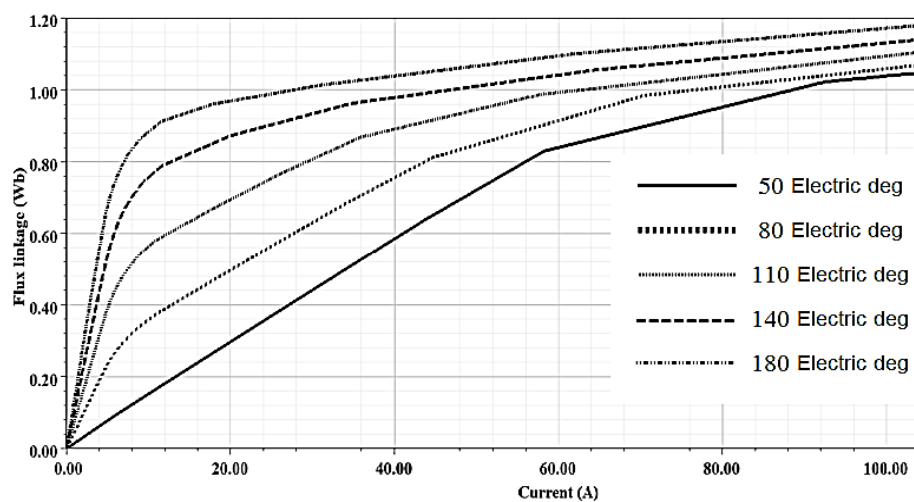


Figure 3. Flux linkage with current characteristic for different rotor positions at speed 3000 rpm

#### 4. THE MATHEMATICAL MODEL OF SRM

The coil's flux linkage ( $\lambda$ ) is directly proportional to both its phase inductance ( $L$ ) and the phase current ( $i$ ) that flows through it, then,

$$V = R_s i + \frac{d\lambda(\theta, i)}{dt} \quad (1)$$

$$\lambda = L(\theta, i) i \quad (2)$$

where  $R_s$  = The resistance per phase,  $\theta$  : Rotor position. Then it requires a partial derivative, in which inductance ( $L$ ) is first assumed as constant and current ( $i$ ) as a variable. The voltage equation for one phase can be expressed by replacing the variable inductance ( $L$ ) in the aforementioned equation and solving it [25].

$$V = R_s i + L(\theta, i) \frac{di}{dt} + \frac{dL(\theta, i)}{dt} i \quad (3)$$

$$V = R_s i + L(\theta, i) \frac{di}{dt} + i \frac{d\theta}{dt} \frac{dL(\theta, i)}{d\theta} \quad (4)$$

Motor angular speed ( $\omega_m$ ) is the derivative of rotor angular position ( $\theta$ ) in terms of time,

$$V = R_s i + L(\theta, i) \frac{di}{dt} + \frac{dL(\theta, i)}{d\theta} \omega_m i \quad (5)$$

SRM is electrically represented by the equations and circuit design, but machine mechanics need to be taken into consideration for the overall modeling. Figure 4 shows the per phase equivalent circuit of the SRM.

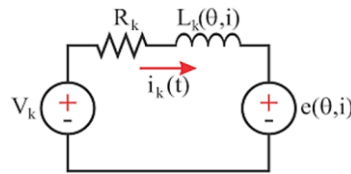


Figure 4. Equivalent circuit per phase of SRM [23]

By using Faraday's law of electromagnetic induction, the electromotive force (emf) induced can be used to generate the torque equation [26].

$$e = - \frac{d\varphi(i, \theta)}{dt} \quad (6)$$

Where  $\varphi(i, \theta)$  = the flux linkage, which depends on the current and rotor angle, then

$$\frac{d\varphi(i, \theta)}{dt} = L \frac{di}{dt} + i \frac{dL}{d\theta} \frac{d\theta}{dt} + \omega_m i \frac{dL}{d\theta} \quad (7)$$

The expression for power ( $p$ ) developed reads as (8).

$$P = Li \frac{di}{dt} + \omega_m i^2 \frac{dL}{d\theta} \quad (8)$$

The expression for energy kept in a magnetic field ( $W_e$ ) is (9).

$$W_e = \frac{1}{2} Li^2 \quad (9)$$

Power produced by changes in the magnetic field is provided by (10).

$$\frac{dW_e}{dt} = \frac{1}{2} L 2i \frac{di}{dt} + \frac{1}{2} i^2 \frac{dL}{dt} \quad (10)$$

$$\frac{dW_e}{dt} = Li \frac{di}{dt} + \frac{1}{2} i^2 \frac{dL}{d\theta} \omega_m \quad (11)$$

Where  $P_m$  is the difference between the power from the supply and the power produced by the magnetic field changing, and it is provided by (12).

$$P_m = \frac{1}{2} \omega_m i^2 \frac{dL}{d\theta} \quad (12)$$

Knowing that the torque (T) is determined by ( $P_m/\omega_m$ ),

$$T = \frac{1}{2} i^2 \frac{dL}{d\theta} \quad (13)$$

where  $T$  = Torque,  $i$  = phase current,  $\frac{dL}{d\theta}$  = rate of change of inductance with the position.

This demonstrates that the torque is directly related to the current squared, and the rate of inductance change with the position. In literature, the SRM efficiency is frequently employed as an objective function to enhance machine performance. The main loss causes in SRMs are copper losses ( $P_{cu}$ ), rotor windage losses ( $P_{win}$ ), and core losses ( $P_{core}$ ). The efficiency of the SRM can be enhanced by reducing these losses, as shown in (14).

$$\eta = \frac{P_{mech}}{P_{elec}} = \frac{P_{mech}}{P_{mech} + P_{cu} + P_{core} + P_{win} + P_{other}} \quad (14)$$

Where  $P_{mech}$  is the output mechanical power,  $P_{elec}$  is the input electrical power,  $P_{other}$  is the other losses unrelated to the electromagnetic design, such as the bearing friction loss, and  $\eta$  is the SRM efficiency. Because to the salient nature of the rotor construction, the rotor windage loss is taken into account as an electromagnetically dependent parameter in this equation.

## 5. METHOD AND PROPOSED MODEL OF SRM

Studies in the domains of electromagnetism, winding configurations, magnetic circuit behavior, inductance, and winding resistance are all part of the general theory that directs the design of an electric machine [27]. All of these studies and the empirical knowledge that designers and researchers have accumulated over the years are taken into consideration when constructing an electric machine. This section presents the proposed optimization method for the most important topology parameters in enhancing the output characteristics. The optimization technique requires the selection of design variables, objective functions, and constraints of the chosen design parameters. Table 1 displays initial design parameters of conventional SRM with FE analysis. For the effective design of SRM, some design guidelines should be followed. The design tenet for the stator/rotor pole arc angle is as follows. The stator/rotor pole arc values are chosen to determine the motor torque profile and to ensure proper machine starting. The SRM project incorporates these needs by setting a lower and higher limit for the polar arc values. To ensure proper machine starting and avoid parasitic currents brought on by the magnetic flux dispersion effect, the polar arc of the rotor must be bigger than the polar arc of the stator [28].

$$\beta_r \geq \beta_s \quad (15)$$

Where  $\beta_r$  = rotor pole arc and  $\beta_s$  = stator pole arc. According on the number of poles on the machine, the (3) determines the minimal value for polar arcs.

$$\text{Min}(\beta_s, \beta_r) = \frac{4\pi}{N_s N_r} \quad (16)$$

Where  $N_r$  = the number of rotor poles,  $N_s$  = the number of stator poles.

The angle between the corners of the adjacent rotor poles must be greater than the stator's polar arc in order to prevent the overlap of the stator and rotor poles in the nonaligned state [5]. As a result, it is possible that the lowest inductance value will rise, reducing the gap between the maximum and minimum values and consequently lowering the torque value. The (4) presents this relationship.

$$\frac{2\pi}{N_r} - \beta_r > \beta_s \quad (17)$$

Table 1. Switched reluctance motor design specifications

| Parameter                    | Value     | Unit |
|------------------------------|-----------|------|
| Outer diameter (Stator)      | 176.4     | mm   |
| Inner diameter (Stator)      | 116.8     | mm   |
| Back iron thickness (Stator) | 13.8      | mm   |
| Air-gap length               | 0.35      | mm   |
| Outer diameter (Rotor)       | 116.1     | mm   |
| Stator/rotor poles           | 8/6       |      |
| Stator/rotor pole arc        | 20.2/23.5 | deg  |
| Stator/rotor pole height     | 16/16     | mm   |
| Number of turns/poles        | 75        |      |
| Slot fill factor             | 0.9       |      |
| Height of the coil           | 9.6       | mm   |
| Stack length                 | 171       | mm   |
| Stator/rotor core material   | M19 steel |      |
| power                        | 5         | KW   |
| speed                        | 3000      | rpm  |

Considering the design criteria in Table 1, when  $\beta_s=20.2^\circ$ , then  $20.2^\circ \leq \beta_r \leq 39.8^\circ$ . The stator pole arc coefficients and rotor pole arc coefficient can be used to indicate the stator pole arc and rotor pole arc [11], respectively.

$$\begin{cases} \alpha_s = \beta_s / \theta_s \\ \alpha_r = \beta_r / \theta_r \end{cases} \quad (18)$$

Where  $\alpha_r$  = Rotor pole arc coefficient,  $\alpha_s$  = Stator pole arc coefficient.

According to (15)-(17), the pole arc coefficients estimated ranges. The objective function of maximum torque, average torque, and efficiency is optimized using a genetic algorithm (GA), with stator/rotor pole arc as variables of GA optimization techniques. In the 1970s, the genetic algorithm (GA) was initially developed [29]. It imitates the way that species evolve and the idea of natural selection. This is primarily accomplished through the processes of parental selection, crossover, and mutation, as shown in Figure 5. The fitness value of the parents is used to determine the initial values (parameters) for them (objective function value). High-fit individuals are used to develop offspring from their chromosomes as part of the selection process, which is often based on a probability function. In other words, the community's most fit individuals have the best chance of giving product to the following generation. The algorithm converts the parent values from numbers to binary strings. The binary strings of every variable are linked to a chromosome. Figure 5 depicts the crossover breeding process between the blue and red parent strings, which produce progeny by sharing their chromosomes. After that, each child string is mutated to choose a random bit and flip it.

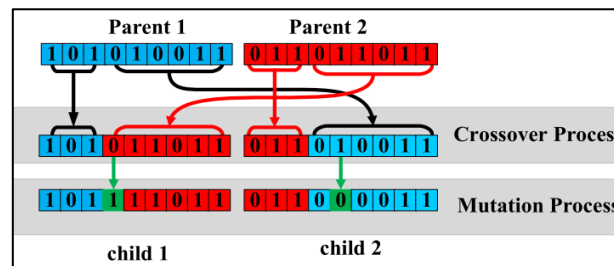


Figure 5. The GA optimization technique's crossover and mutation processes [30]

A flow chart of the proposed design with GA process is shown in Figure 6. The conventional SRM is designed according to the initial design data shown in Table 1 using Ansys electronics desktop software. The electromagnetic performance of a conventional SRM is analyzed with the torque characteristics and magnetic flux density vector plot are displayed. The proposed analysis focuses on changing the parameters of the topology that have the most effect on improving the torque and efficiency of the motor, which includes the angle of the stator/rotor pole arc. The various output, parameters for flux distribution, losses, efficiency, and torque change when the polar arcs shift. Iterative genetic algorithm (GA) optimization can be used to determine

the ideal value for the polar arc's parameters. With an initial population of  $m$ , the algorithm begins. Each of these design points (individuals) has a computed fitness. In the  $k^{\text{th}}$  generation, two people are selected to serve as parents. The crossover method is then applied to all of the highly fit people with a high probability of up to 0.9. The crossover results in the production of two children. The use of the high fitness individuals to produce offspring is regulated by the crossover probability,  $r_c$ . In the absence of a crossover, on the other hand, the two children will be exact replicas of their parents. Then, each of the two children receives the mutation with a minimum chance of up to 0.01. The exploration process is governed by the mutation probability  $r_m$ , which also prohibits an early convergence to a local optimal solution.

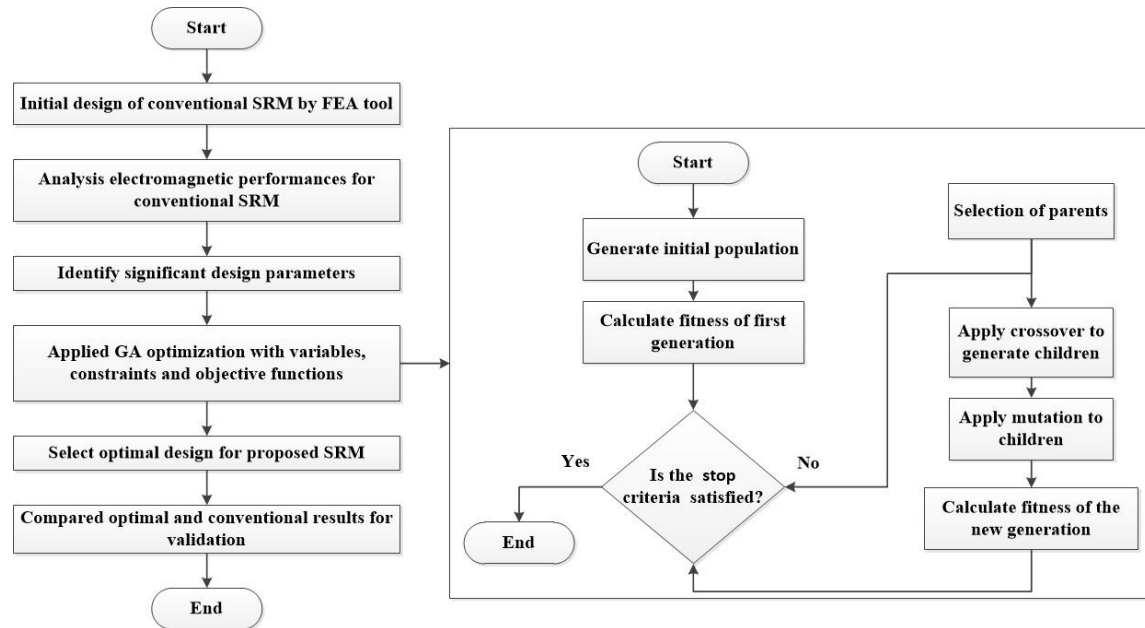


Figure 6. A flowchart of proposed design optimization

The new one replaces the old population, and each member of the new population is assessed for fitness. Up until the termination condition is met, the processes of crossover and mutation are repeated [29]. The GA directly influences how the population is formed for a new generation by  $r_c$  and  $r_m$ . Therefore, the variation of the stator/rotor pole arc angle according to the conditions in (15)-(17) with ranges  $(15^\circ \leq \beta_s \leq 29.9^\circ) - (15^\circ \leq \beta_r \leq 30^\circ)$  that ensure the desired results. After GA optimization is completed, the optimal results are selected and compared with the conventional results for validation.

## 6. RESULTS AND DISCUSSION

To ensure that the simulation and the aforementioned analyses are accurate. The results of the conventional parameters as shown in the Table 2 as well as the results of the optimization parameters (stator/rotor pole arc) are presented. To showing the improvement of the maximum torque, average torque. In addition, the efficiency improvement in most of the cases presented.

### 6.1. The conventional parameters of SRM

The magnetic flux lines and flux density distribution in the yoke and air gap are evidently different when the stator and rotor are in various relative positions. The Figure 7 shows a plot of the magnitude and vector of the magnetic field density, as it indicates the path of the magnetic flux flow during the rotation of the motor at speeds (50% and 100%) of rated speed. Where it shows the conditions for fully alignment and non-alignment of the stator/rotor pole. In Figure 7(a), shows the variance in the magnetic field densities achieves its maximum value in the corners of the stator/rotor pole in fully alignment condition at speeds (1500 rpm, 3000 rpm) respectively. The stator and rotor teeth have the smallest air gap when they are aligned, as shown in Figure 7(a). Reluctance is at its smallest and inductance is at its largest at this position. So, the output torque is increased in this position.

While in Figure 7(b), shows the variance in the magnetic field densities achieves its maximum value in the corners of the stator/rotor pole in non-alignment condition at speeds (1500 rpm, 3000 rpm) respectively.

The effective air gap between the teeth of both the stator and rotor is at its greatest in the non-aligned position, as demonstrated in Figure 7(b). The reluctance is greatest and the inductance is smallest at this position. Therefore, the output torque is increased in this position. As the rotor poles and the main stator poles are not aligned in the non-aligned, the flux value is nearly entirely dictated by the winding and the air around it. In contrast to the aligned position, no saturation happens in the non-aligned position even at larger current ratings.

Table 2. Values of torque and efficiency at different of the stator/rotor pole arc

| Speed (rpm) | Cases        | $\beta_r$ (deg) | $\beta_s$ (deg) | Tmax(N.m) | Tavg(N.m) | Efficiency  |
|-------------|--------------|-----------------|-----------------|-----------|-----------|-------------|
| 900         | Case 1(Con)  | 23.5            | 20.2            | 37.3548   | 17.7199   | 91.41838892 |
|             | Case 2 (Opt) | 26.65135655     | 15.83492869     | 41.5988   | 19.4226   | 89.76940484 |
|             | Case 3 (Opt) | 24.05941954     | 17.00702742     | 45.3688   | 19.1513   | 90.30847068 |
|             | Case 4 (Opt) | 24.2178106      | 16.42662342     | 46.315    | 19.3379   | 90.12035104 |
|             | Case 5 (Opt) | 21.27887814     | 21.08084101     | 40.8467   | 18.8155   | 90.68271095 |
|             | Case 6 (Opt) | 21.49861141     | 18.68293635     | 47.5312   | 19.9518   | 91.74068055 |
| 1500        | Case 1(Con)  | 23.5            | 20.2            | 18.1988   | 6.453     | 93.73743278 |
|             | Case 2 (Opt) | 26.65135655     | 15.83492869     | 21.3861   | 7.552     | 94.14429549 |
|             | Case 3 (Opt) | 24.05941954     | 17.00702742     | 21.5752   | 8.2961    | 93.92567425 |
|             | Case 4 (Opt) | 24.2178106      | 16.42662342     | 22.4859   | 8.5596    | 93.91686899 |
|             | Case 5 (Opt) | 21.27887814     | 21.08084101     | 19.7397   | 7.6077    | 93.98434345 |
|             | Case 6 (Opt) | 21.49861141     | 18.68293635     | 24.7484   | 9.3695    | 94.31617625 |
| 2250        | Case 1(Con)  | 23.5            | 20.2            | 9.1066    | 2.9005    | 93.59091035 |
|             | Case 2 (Opt) | 26.65135655     | 15.83492869     | 11.1312   | 3.3434    | 94.12164302 |
|             | Case 3 (Opt) | 24.05941954     | 17.00702742     | 10.5835   | 3.7316    | 94.17331721 |
|             | Case 4 (Opt) | 24.2178106      | 16.42662342     | 11.4623   | 3.8658    | 94.21777532 |
|             | Case 5 (Opt) | 21.27887814     | 21.08084101     | 9.7407    | 3.4425    | 94.13893673 |
|             | Case 6 (Opt) | 21.49861141     | 18.68293635     | 13.6077   | 4.2891    | 94.60771831 |
| 3000        | Case 1(Con)  | 23.5            | 20.2            | 5.2508    | 1.7289    | 93.46123496 |
|             | Case 2 (Opt) | 26.65135655     | 15.83492869     | 6.5197    | 1.9997    | 93.97179235 |
|             | Case 3 (Opt) | 24.05941954     | 17.00702742     | 6.1916    | 2.2396    | 94.16480801 |
|             | Case 4 (Opt) | 24.2178106      | 16.42662342     | 6.73      | 2.3229    | 94.25257622 |
|             | Case 5 (Opt) | 21.27887814     | 21.08084101     | 5.6722    | 2.0619    | 94.04731175 |
|             | Case 6 (Opt) | 21.49861141     | 18.68293635     | 8.4088    | 2.5748    | 94.66352466 |

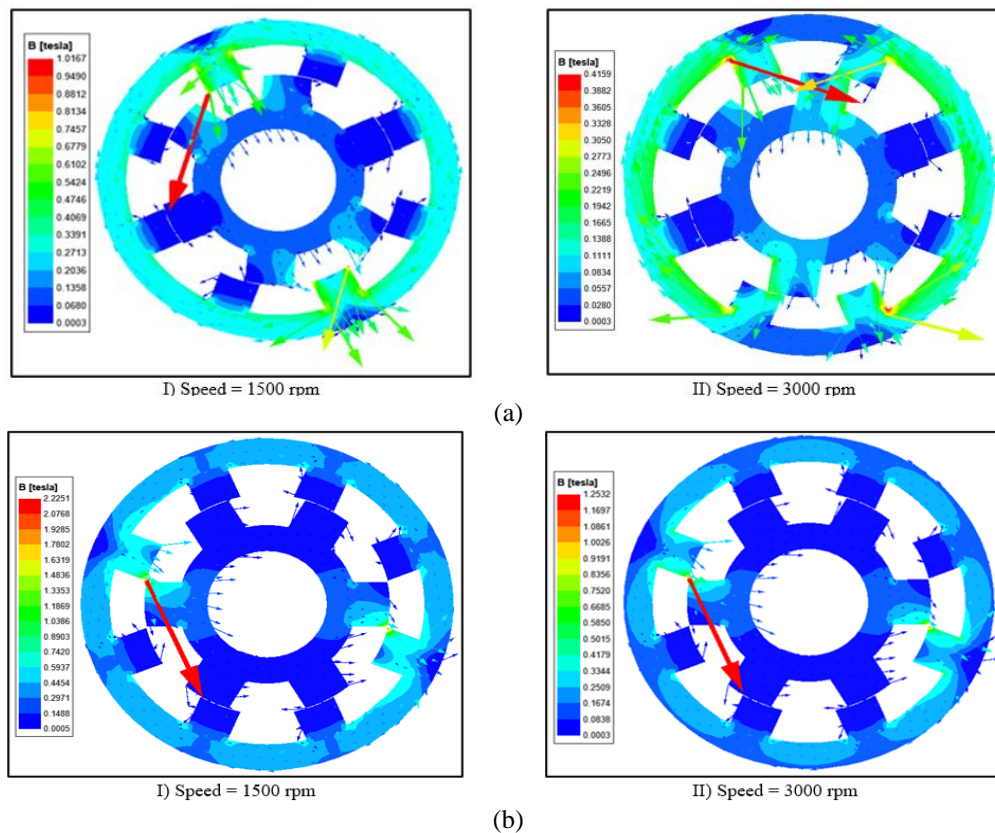


Figure 7. Orientation of magnetic field lines of conventional SRM at (a) alignment condition and (b) non-alignment condition



## 6.2. The optimization parameters of SRM

The stator/rotor pole's arc angle is the only variable that is altered in the SRM's optimized parameters. The optimization parameters' finite element analysis reveals a change in the output values with regard to torque and efficiency for the same set of additional parameters as in the traditional analysis. The torque and efficiency values are variable for the various stator/rotor pole arc angle values, as shown in Table 2.

Table 2 displays the top optimum 5 cases for the maximum/average torque values and efficiency determined by the (FE) analysis at speeds that are (30%, 50%, 70%, and 100%) of the rated speed. From Table 2 in comparison with conventional model, the best optimal case obtained at ( $\beta_r=21.49861141^\circ$ ,  $\beta_s=18.68293635^\circ$ ). It is observed that the maximum torque with values [47.5312, 24.7484, 13.6077, 8.4088 (N.m)] increased with [10.17, 6.54, 4.5, 3.15 (N.m)], average torque with values [19.9518, 9.3695, 4.2891, 2.5748 (N.m)] increased with [2.23, 2.91, 1.38, 0.84 (N.m)] for speeds [900, 1500, 2250, 3000 (rpm)] respectively. At same best optimal values of ( $\beta_r, \beta_s$ ) the efficiency with values [91.74068055, 94.31617625, 94.60771831, 94.66352466] increased with [0.32, 0.57, 1.01, 1.2] for speeds [900, 1500, 2250, 3000 (rpm)] respectively. The comparison between the conventional and best optimum results of maximum/average torque and efficiency shown in Figure 8.

Figure 8(a) displays the best optimum value of Tmax compared with conventional model for speeds (900, 1500, 2250, and 3000) rpm. Figure 8(b) displays the best optimum value of Tavg compared with conventional model for speeds (900, 1500, 2250, and 3000) rpm. Figure 8(c) displays the best optimum value of the efficiency compared with conventional model for speeds (900, 1500, 2250, and 3000) rpm. Figure 9 shows torque profile plot in non-alignment condition and rotor position  $22.5^\circ$  at speeds ((30%, 50%, 70%, and 100%) of rated speed for the conventional and optimization parameters of SRM.

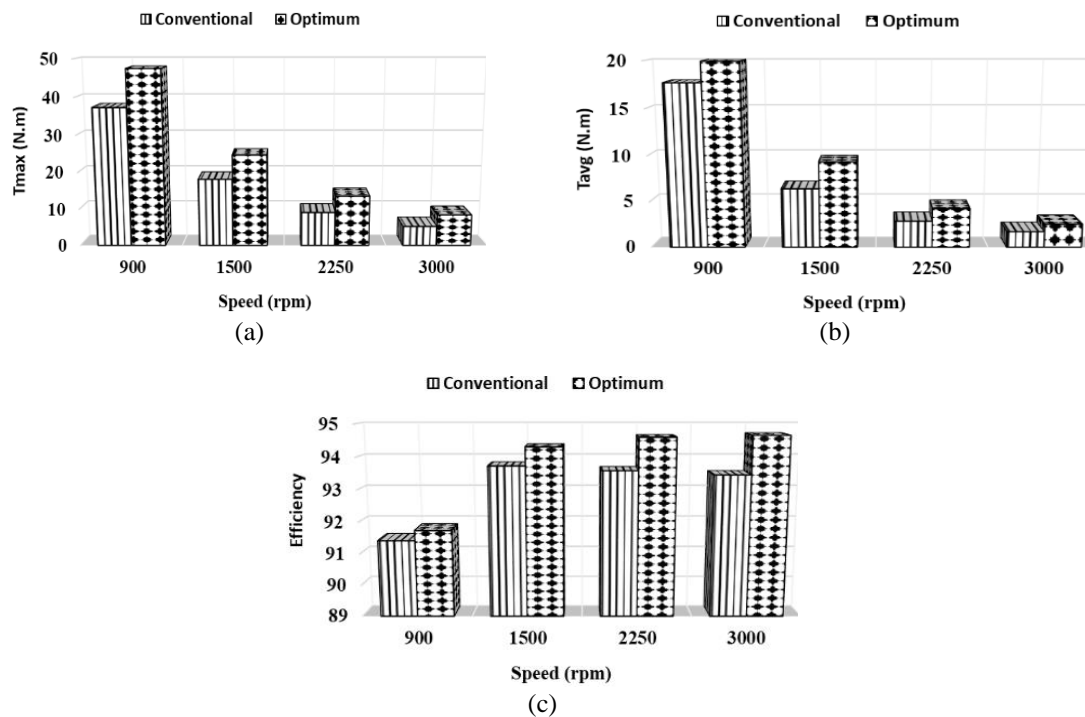


Figure 8. The comparison between conventional and best optimum values of results (a) maximum torque, (b) average torque, and (c) efficiency

From the Figure 9(a), at speed = 900 rpm, it is observed that the best optimum value of Tmax = 47.5312 N.m, Tavg = 19.9518 N.m and the maximum efficiency = 91.74068055 occur at ( $\beta_r = 21.49861141^\circ$ ,  $\beta_s = 18.68293635^\circ$ ). For Figure 9(b), at speed = 1500 rpm, it has been noted that the best optimum value of Tmax = 24.7484 N.m, Tavg = 9.3695 N.m and the efficiency = 94.31617625 occur at ( $\beta_r = 21.49861141^\circ$ ,  $\beta_s = 18.68293635^\circ$ ). While Figure 9(c), at speed = 2250 rpm, it has been noted that the best optimum value of Tmax = 13.6077 N.m, Tavg = 4.2891 N.m and the efficiency = 94.60771831 occur at ( $\beta_r = 21.49861141^\circ$ ,  $\beta_s = 18.68293635^\circ$ ). Therefore Figure 9(d), at speed = 3000 rpm, it has been noted that the best optimum value of Tmax = 8.4088 N.m, Tavg = 2.5748 N.m and the efficiency = 94.66352466 occur at ( $\beta_r = 21.49861141^\circ$ ,  $\beta_s = 18.68293635^\circ$ ).

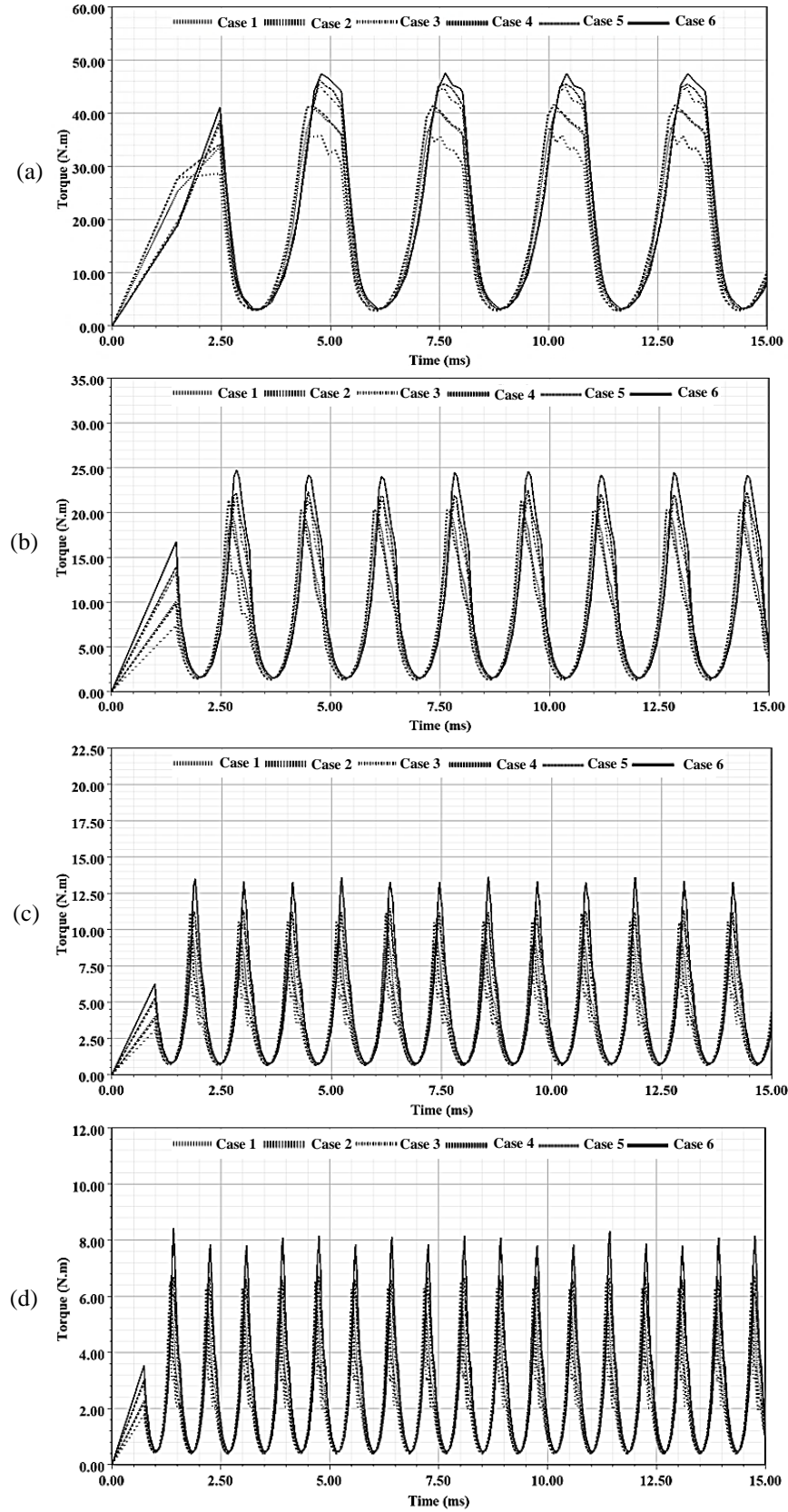


Figure 9. Torque profile of the conventional and optimization parameters at non-alignment condition and rotor position  $22.5^\circ$  for (a) speed = 900 rpm, (b) speed = 1500 rpm, (c) speed = 2250 rpm, and (d) speed = 3000 rpm

## 7. CONCLUSION

SRM's benefits, including its high overload capacity, superior fault tolerance, and wide speed range, make it ideal for use in EV and HEVs. In this paper, optimization was carried out by the genetic algorithm (GA) on the topology parameters of an 8/6 SRM. Which change the shape of the stator and rotor poles, including the arcs of the stator and rotor poles, according to conditions restricted by finite element (FE) analysis. The maximum torque has been improved (27.24 %, 35.98%, 49.42%, 60.14%), the average torque has been improved (12.59%, 45.19%, 47.87%, 48.92%) and the efficiency has been improved (0.35%, 0.61%, 1.08%, 1.28%) for speeds [900, 1500, 2250, 3000 (rpm)] respectively. A 2D model is developed for performance evaluation of machine. The results of the improved parameters were compared with the conventional ones at different motor speeds. The effect of the stator/rotor pole arc angle is evident on improving the torque and efficiency of the SRM. Which gives high confidence to use it and reduces the interest in the permanent magnet motor in electric vehicle application.




## REFERENCES

- [1] N. R. Patel, V. A. Shah, and M. M. Lokhande, "A novel approach to the design and development of 12/15 radial field c-core switched reluctance motor for implementation in electric vehicle application," *IEEE Transactions on Vehicular Technology*, vol. 67, no. 9, pp. 8031–8040, 2018, doi: 10.1109/TVT.2018.2839695.
- [2] E. Öksüztepe, "In-Wheel Switched Reluctance Motor Design for Electric Vehicles by Using a Pareto-Based Multiobjective Differential Evolution Algorithm," *IEEE Transactions on Vehicular Technology*, vol. 66, no. 6, pp. 4706–4715, 2017, doi: 10.1109/TVT.2016.2618119.
- [3] Z. Shi *et al.*, "Torque Analysis and Dynamic Performance Improvement of a PMSM for EVs by Skew Angle Optimization," *IEEE Transactions on Applied Superconductivity*, vol. 29, no. 2, pp. 1–5, 2019, doi: 10.1109/TASC.2018.2882419.
- [4] A. Siadatan, N. Fatahi, and M. Sedaghat, "Optimum Designed Multilayer Switched Reluctance Motors for use in Electric Vehicles to Increase Efficiency," *SPEEDAM 2018 - Proceedings: International Symposium on Power Electronics, Electrical Drives, Automation and Motion*, pp. 304–308, 2018, doi: 10.1109/SPEEDAM.2018.8445215.
- [5] R. Li, Sufe; Zhang, Shen; Habetler, Thomas; Harley, "Modeling, Design Optimization and Applications of Switched Reluctance Machines - A Review. IEEE Transactions on Industry Applications," *IEEE Transactions on Industry Applications*, vol. 55, no. 3, pp. 2660–2681, 2019, doi: 10.1109/TIA.2019.2897965.
- [6] G. Davarpanah and J. Faiz, "A Novel Structure of Switched Reluctance Machine with Higher Mean Torque and Lower Torque Ripple," *IEEE Transactions on Energy Conversion*, vol. 35, no. 4, pp. 1859–1867, 2020, doi: 10.1109/TEC.2020.2990914.
- [7] A. Xu, C. Shang, J. Chen, J. Zhu, and L. Han, "A New Control Method Based on DTC and MPC to Reduce Torque Ripple in SRM," *IEEE Access*, vol. 7, no. c, pp. 68584–68593, 2019, doi: 10.1109/ACCESS.2019.2917317.
- [8] M. Zhang, I. Bahri, X. Mininger, C. Vlad, and E. Berthelot, "Vibration reduction control of switched reluctance machine," *IEEE Transactions on Energy Conversion*, vol. 34, no. 3, pp. 1380–1390, 2019, doi: 10.1109/TEC.2019.2908458.
- [9] O. S. A. Alyozbaky, M. Zainal, and A. Ab, "Influence of non-sinusoidal power supply on the performance of a single-phase capacitor induction motor," vol. 25, no. 3, pp. 1246–1257, 2022, doi: 10.11591/ijeecs.v25.i3.pp1246-1257.
- [10] M. A. Al-yoonus and O. S. A. Alyozbaky, "Detection of internal and external faults of single-phase induction motor using current signature," vol. 11, no. 4, pp. 2830–2841, 2021, doi: 10.11591/ijece.v11i4.pp2830-2841.
- [11] X. Sun, K. Diao, G. Lei, Y. Guo, and J. Zhu, "Study on segmented-rotor switched reluctance motors with different rotor pole numbers for bsg system of hybrid electric vehicles," *IEEE Transactions on Vehicular Technology*, vol. 68, no. 6, pp. 5537–5547, 2019, doi: 10.1109/TVT.2019.2913279.
- [12] Y. Li, S. Ravi, and Di. C. Aliprantis, "Tooth shape optimization of switched reluctance motors for improved torque profiles," *Proceedings - 2015 IEEE International Electric Machines and Drives Conference, IEMDC 2015*, no. 1, pp. 569–575, 2016, doi: 10.1109/IEMDC.2015.7409115.
- [13] X. Sun, Y. Shen, S. Wang, G. Lei, Z. Yang, and S. Han, "Core Losses Analysis of a Novel 16/10 Segmented Rotor Switched Reluctance BSG Motor for HEVs Using Nonlinear Lumped Parameter Equivalent Circuit Model," *IEEE/ASME Transactions on Mechatronics*, vol. 23, no. 2, pp. 747–757, 2018, doi: 10.1109/TMECH.2018.2803148.
- [14] H. Eskandari and M. Mirsalim, "An improved 9/12 two-phase e-core switched reluctance machine," *IEEE Transactions on Energy Conversion*, vol. 28, no. 4, pp. 951–958, 2013, doi: 10.1109/TEC.2013.2279344.
- [15] R. V. S. N. B. G. Fernandes, "High torque polyphase segmented switched reluctance motor with novel excitation strategy," no. September 2011, pp. 375–384, 2012, doi: 10.1049/iet-epa.2011.0285.
- [16] H. Torkaman, E. Afjei, and M. S. Toulabi, "New Double-Layer-per-Phase Isolated Switched Reluctance Motor: Concept , Numerical Analysis , and Experimental Confirmation," vol. 59, no. 2, pp. 830–838, 2012.
- [17] H. Arihara and K. Akatsu, "Basic Properties of an Axial-Type Switched Reluctance Motor," *IEEE TRANSACTIONS ON INDUSTRY APPLICATIONS*, vol. 49, no. 1, pp. 59–65, 2013, doi: 10.1109/TIA.2012.2229683.
- [18] Y. Ebrahimi and M. R. Feyzi, "Introductory assessment of a novel high-torque density axial flux switched reluctance machine," *IET Electric Power Applications Research, Article Introductory*, vol. 11, ss.7, pp. 1315–1323, 2017, doi: 10.1049/iet-epa.2017.0081.
- [19] J. Zhu, K. W. E. Cheng, X. Xue, and Y. Zou, "Design of a New Enhanced Torque In-Wheel Switched Reluctance Motor with Divided Teeth for Electric Vehicles," *IEEE Transactions on Magnetics*, vol. 53, no. 11, 2017, doi: 10.1109/TMAG.2017.2703849.
- [20] Z. Ling, J. Ji, T. Zeng, and W. Zhao, "Design optimization and comparison of linear magnetic actuators with different topologies," *Chinese Journal of Electrical Engineering*, vol. 6, no. 1, pp. 41–51, 2020, doi: 10.23919/CJEE.2020.000003.
- [21] C. Ma and L. Qu, "Multiobjective optimization of switched reluctance motors based on design of experiments and particle swarm optimization," *IEEE Transactions on Energy Conversion*, vol. 30, no. 3, pp. 1144–1153, 2015, doi: 10.1109/TEC.2015.2411677.
- [22] G. Bramerdorfer, J. A. Tapia, J. J. Pyrhonen, and A. Cavagnino, "Modern Electrical Machine Design Optimization: Techniques, Trends, and Best Practices," *IEEE Transactions on Industrial Electronics*, vol. 65, no. 10, pp. 7672–7684, 2018, doi: 10.1109/TIE.2018.2801805.
- [23] Vuddanti Sandeep; Vinod Karknalli; and Surender Reddy Salkuti, "Design and comparative analysis of three phase, four phase and six phase switched reluctance motor topologies for electrical vehicle propulsion," *Bulletin of Electrical Engineering and Informatics*, vol. 10, no. 3, pp. 1495–1504, 2021, doi: 10.11591/eei.v10i3.3054.




- [24] M. Suresh, R. Meenakumari, H. Panchal, E. Sayed, and E. Agouz, "An Enhanced Multiobjective Particle Swarm Optimization algorithm for optimum utilization of Hybrid Renewable Energy Systems An Enhanced Multiobjective Particle Swarm Optimization algorithm for optimum utilization of Hybrid Renewable Energy Systems," *International Journal of Ambient Energy*, vol. 0, no. 0, pp. 1–10, 2020, doi: 10.1080/01430750.2020.1737837.
- [25] S. Narasimha; S. R. Salkuti, "Design and implementation of smart uninterruptible power supply using battery storage and photovoltaic arrays," *International Journal of Engineering & Technology*, vol. 7, no. 3, pp. 960–965, 2018, doi: 10.14419/ijet.v7i3.12305.
- [26] S. Narasimha; S. R. Salkuti, "Design and operation of closed-loop triple-deck buck-boost converter with high gain soft switching," *International Journal of Power Electronics and Drive System (IJPEDS)*, vol. 11, no. 1, pp. 523–529, 2020, doi: 10.11591/ijpeds.v11.i1.pp523-529.
- [27] Pyrhönen J; Jokinen T; and Hrabovcová V, *Design of Rotating Electrical Machines*, 2nd ed. Chichester: John Wiley & Sons, 2014.
- [28] Patel; Nikunj R.; and Jiten K. Chavda, "Design and Performance Analysis of 8/6 Radial Field Switched Reluctance Motor for Electric Vehicle Application," *UGC CARE APPROVED JOURNAL*, vol. 26, no. 3, pp. 2013–2015, 2021.
- [29] A. Lambora, K. Gupta, and K. Chopra, "Genetic Algorithm- A Literature Review," in *2019 International Conference on Machine Learning, Big Data, Cloud and Parallel Computing (COMITCon)*, Faridabad, India, 2019, no. 1998, pp. 380–384, doi: 10.1109/COMITCon.2019.8862255.
- [30] M. Abdalmagid, E. Sayed, M. H. Bakr, and A. Emadi, "Geometry and Topology Optimization of Switched Reluctance Machines: A Review," *IEEE Access*, vol. 10, pp. 5141–5170, 2022, doi: 10.1109/ACCESS.2022.3140440.

## BIOGRAPHIES OF AUTHORS



**Saif Kh Al-Farhan**    was born in Ninawa, Iraq, in 1991. He received his Bachelor of Science (BSc) degree in Electrical Engineering from the Electrical Engineering Department, College of Engineering, University of Mosul, Iraq, in 2013. Then he was appointed assistant engineer at the Iraqi Ministry of Oil - State Company for Gas Filling and Services, where his work focuses on the various electrical machines used in liquid gas filling plants. Where he is currently pursuing the M.Sc. degree. His main research interest includes optimization, SRM design and control for automobile application. He can be contacted at email: saif.21enp17@student.uomosul.edu.iq.



**Omar Sharaf Al-Deen Yehya Al-Yozbaky**    he obtained his Bachelor of Science (BSc) in Electrical Engineering in 2001 from the Electrical Engineering Department, College of Engineering, University of Mosul, Iraq. Then he was appointed as an assistant engineer in the same mentioned department. After that, he got MSc in "Overcome the effect of Critical distance in XLPE High Voltage Cables by inductive shunt compensator", 2008 from the same mentioned department as well. Upon his graduation, he was appointed as teaching staff (assistant lecturer) in the Electrical Engineering Department, College of Engineering, University of Mosul. In 2012, he obtained the scientific title (lecturer) and the Ph.D. degree in the Department of Electrical and Electronic Engineering, Faculty of Engineering, University Putra Malaysia in 2017. Since 2014, he was a member of the Centre for Electromagnetic and lightning protection research (CELP). Now, he is Assistant Professor Electrical Engineering Department, College of Engineering, University of Mosul. The subjects for interest, Renewable energy fields associated with the smart grid, thermal modeling transformer design, and electrical machines. He can be contacted at email: o.yehya@uomosul.edu.iq.